Journal of Statistical Physics, Vol. 82, Nos. 5/6, 1996

Dynamics and Growth of Particles Undergoing Ballistic Coalescence

Emmanuel Trizac[1] and Jean-Pierre Hansen[2, 3]

Received May 30, 1995; final August 15, 1995

The irreversible evolution of a model for ballistic coalescence of spherical particles, whereby colliding particles merge into a single, larger sphere with conservation of mass and momentum, is analyzed on the basis of scaling assumptions, mean-field theory, and kinetic theory for arbitrary dimensionality and size–mass relation. The asymptotic growth regime is characterized by scaling laws associated with the instantaneous mean mass and kinetic energy of the particles. A hyperscaling relation between the mass and energy exponents is derived. The predictions of the theoretical analysis are tested by extensive simulations of the two-dimensional version of the model. Due to multiple coalescence events, the exponents are found to be nonuniversal (i.e., density dependent) and to differ significantly from the mean-field predictions. The distribution of masses turns out to be universal and exponential. Particle energies follow a Boltzmann distribution, with a time-dependent temperature, or relax toward such a distribution, even when the initial distribution is highly non-Maxwellian. In the case where the particles are "swollen" [i.e., the size–mass relation involves the Flory exponent $\nu = 3/(d+2)$], an asymptotic scaling regime is observed only for sufficiently low initial packing fractions. At higher densities, the irreversible evolution terminates in a "catastrophic" coalescence event involving all remaining particles.

KEY WORDS: Coalescence; aggregation; dynamic scaling; asymptotic growth; kinetic theory; molecular dynamics.

[1] Laboratoire de Physique, Unité de Recherche Associée 1325 du Centre National de la Recherche Scientifique, École Normale Supérieure de Lyon, 69364 Lyon Cedex 07, France. E-mail: etrizac@physique.ens-lyon.fr.

[2] Physical and Theoretical Chemistry Laboratory, Oxford University, Oxford OX1 3QZ, Great Britain.

[3] On leave of absence from Laboratoire de Physique, École Normale Supérieure de Lyon, 69364 Lyon Cedex 07, France.

822/82/5-6-9

1. INTRODUCTION

Statistical models of growth through aggregation or coalescence have received widespread theoretical and numerical attention in relation to irreversible phenomena like nucleation, spinodal decomposition, colloidal aggregation, vapor condensation and breath figures, merging of vortices in turbulent flows, or even the formation of planets from interstellar dust. In many of these models, the elementary processes leading to growth are essentially random in nature. This is the case of the widely studied model of diffusion-limited aggregation (DLA)[1] (see ref. 2 for a review), where an eventually fractal object grows via the sequential attachment of random (or Brownian) walkers. In droplet deposition and growth models (see ref. 3 for a recent review) d-dimensional spheres are deposited at random on a $(d-1)$-dimensional surface, where they grow by vapor collection and coalescence; the growing particles retain their spherical shape.

In contrast to random growth, Carnevale *et al.*[4] considered an aggregation model governed by irreversible but deterministic dynamics, whereby d-dimensional spheres move freely within a d-dimensional volume (ballistic motion) until they collide with another sphere; the collisions are fully inelastic, but conserve mass and momentum; upon colliding, two spheres coalesce into a single sphere of diameter $\sigma=(\sigma_1^d+\sigma_2^d)^{1/d}$. The authors deduced the power law governing the asymptotic growth of the mean mass of the particles from a simple mean-field scaling argument, and conjectured an exponential universal distribution of masses in the asymptotic regime. Their predictions were found to agree well with results of simulations on the one-dimensional version of the model. The mean-field argument has been formalized by Jiang and Leyvraz,[5] who also stressed the need of carrying simulations in higher dimensions. Subsequently Piasecki[6] was able to derive the exponential distribution of masses in 1D from kinetic theory, on the basis of a weak mean-field-like assumption. Some rigorous long-time estimates of the mass spectrum were obtained by Martin and Piasecki.[7]

However, an additional complication arises in dimensions higher than one, namely the possibility of multiple coalescence events, involving more than two partners. Such events occur whenever the particle resulting from the coalescence of two spheres coming into contact overlaps additional particles located in the immediate neighborhood of the initial pair. The importance of such events is expected to grow with increasing density, and to depend sensitively on the relation between diameter σ and mass m of the particles (this relation is assumed to be $\sigma \propto m^{1/d}$ in the analysis of Carnevale *et al.*[4])

The purpose of the present work is accordingly two-fold. In a first step, the mean-field scaling analysis of ref. 4 is extended to the case of an arbitrary mass–size relation $\sigma \propto m^{\nu}$. Such a generalization might serve as a crude model for polymerization, where σ may be identified with the radius of gyration of a growing polymer coil and ν could be the Flory exponent (for polymers in good solvent), rather than $1/d$ (corresponding to collapsed polymer chains). Going beyond the mean-field assumption, a careful scaling analysis of the exact kinetic equation governing the distribution function of masses and velocities, valid in the low-density limit, will lead us to a hyperscaling relation between the exponents of the asymptotic power laws governing the growth of the mean mass of the particles and the decrease of the total kinetic energy of the system.

In a second stage, the predictions of the mean-field approximation will be confronted with data of extensive simulations carried out for two-dimensional systems (coalescing disks in a plane), with $\nu = 1/2$ and $\nu = 3/4$. The simulations, which take multiple coalescence events into account properly, clarify the role of the latter, which turns out to be the origin of non-universal scaling behavior.

A preliminary account of parts of this work has appeared elsewhere.[8]

2. THE MODEL FOR BALLISTIC COALESCENCE

Consider a system initially (at time $t = 0$) made up of N_0 identical d-dimensional spheres of diameter σ_0 and mass m_0, in a d-dimensional domain of measure Ω; the initial number density is $n_0 = N_0/\Omega$, and its dimensionless counterpart, which is proportional to the packing fraction, is $n_0^* = n_0 \sigma_0^d$. The N_0 particles are given initial velocities $\{\mathbf{v}_i\}$ sampled from some distribution $\phi_0(\mathbf{v})$. They then undergo free particle (or ballistic) motion, interrupted by a succession of instantaneous, completely inelastic collisions whenever a pair of spheres come into contact (no rotations of the particles are involved). As a result of an inelastic binary collision, the two initial spheres i and j merge into a single sphere with conservation of mass, center of mass (CM), and momentum:

$$m = m_i + m_j \tag{1a}$$

$$\mathbf{r} = \frac{1}{m}(m_i \mathbf{r}_i + m_j \mathbf{r}_j) \tag{1b}$$

$$m\mathbf{v} = m_i \mathbf{v}_i + m_j \mathbf{v}_j \tag{1c}$$

Since the initial relative velocity of the colliding pair, $\mathbf{v}_{ij}=\mathbf{v}_i-\mathbf{v}_j$, vanishes in the inelastic collision, the final kinetic energy $mv^2/2$ is less than the initial kinetic energy:

$$\varepsilon=\tfrac{1}{2}mv^2\leqslant\varepsilon_i+\varepsilon_j=\tfrac{1}{2}m_iv_i^2+\tfrac{1}{2}m_jv_j^2$$

In fact, an elementary calculation shows that

$$\varepsilon_i+\varepsilon_j=\varepsilon+\tfrac{1}{2}\mu v_{ij}^2$$

where $1/\mu=1/m_i+1/m_j$ is the reduced mass, from which it can be deduced that ε is bounded above and below by

$$\frac{1}{m}[\sqrt{m_i\varepsilon_i}-\sqrt{m_j\varepsilon_j}]^2\leqslant\varepsilon\leqslant\varepsilon_i+\varepsilon_j-\frac{1}{m}[\sqrt{m_i\varepsilon_i}-\sqrt{m_j\varepsilon_j}]^2 \tag{2}$$

A diameter–mass relation of the form $\sigma\propto m^\nu$ is assumed, such that, according to the mass conservation (1a), the diameter of the sphere resulting from the coalescence of spheres i and j is given by

$$\sigma=(\sigma_1^{1/\nu}+\sigma_2^{1/\nu})^\nu \tag{3}$$

where physically reasonable values of the exponent are in the range $0\leqslant\nu\leqslant1$. If spheres are to be of constant density, $\nu=1/d$, which is the case of ref. 4. However, in the polymer language, if spheres are to represent polymer coils of radius of gyration σ, ν can take the values $1/d$ (collapsed chain), 1/2 (Gaussian chain), or $3/(d+2)$, which is Flory's estimate of the exponent for a "swollen" (self-avoiding) chain.[9]

From the above characteristics of the model it is clear that the total number of particles $N(t)$ and the total kinetic energy of the system

$$K(t)=\sum_{i=1}^{N(t)}\varepsilon_i \tag{4}$$

must be decreasing functions of time. On the other hand, the instantaneous mean mass

$$\langle m\rangle(t)=\frac{1}{N(t)}\sum_{i=1}^{N(t)}m_i=\frac{N_0m_0}{N(t)} \tag{5}$$

increases with time; conservation of mass [Eq. (1a)] was exploited in going from the first to the second equality in Eq. (5). The mean kinetic energy per particle defines an instantaneous kinetic temperature $T(t)$:

$$\langle\varepsilon\rangle(t)=\frac{1}{N(t)}\sum_{i=1}^{N(t)}\varepsilon_i=\frac{K(t)}{N(t)}=\frac{d}{2}k_BT(t) \tag{6}$$

Since both $K(t)$ and $N(t)$ are decreasing functions of time, it is not clear, *a priori*, how $\langle \varepsilon \rangle(t)$ will vary in time.

The mean-field analysis which will be discussed in Section 3 and the 1D simulations of Carnevale *et al.*, as well as the 2D simulations to be presented in Sections 6 and 7, point to an asymptotic power-law (or scaling) behavior of the mean mass and of the total kinetic energy. For sufficiently long times, this translates into

$$\langle m \rangle(t) \propto t^{\xi} \tag{7a}$$

$$K(t) \propto t^{-\delta} \tag{7b}$$

where ξ and $\delta > 0$ are the basic dynamical exponents. According to Eqs. (5) and (6), it follows that

$$N(t) \propto t^{-\xi} \tag{8a}$$

$$\langle \varepsilon \rangle(t) \propto t^{\xi - \delta} \tag{8b}$$

A key objective of the remainder of this paper will be to search for a possible scaling relation between the two fundamental exponents ξ and δ and to determine their numerical values.

The basic time scale in the subsequent analysis is the Boltzmann mean collision time τ_B, i.e., the mean time between two collisions suffered by any one particle. If $a(t) = n(t)^{-1/d}$ denotes the mean spacing between particles at time t [$n(t) = N(t)/\Omega$ is the instantaneous number density] and $\langle v \rangle(t)$ the r.m.s. velocity of particles, the usual kinetic argument[10] shows that τ_B is proportional to

$$\tau_B \propto \frac{[a(t)]^d}{\langle v \rangle(t) \langle \sigma \rangle(t)^{d-1}} \propto \frac{1}{n(t) \langle v \rangle(t) \langle m \rangle^{\nu(d-1)}} \tag{9}$$

where $\langle \sigma \rangle^{d-1}$ is proportional to the binary collision cross selection. Strictly speaking, τ_B is properly defined for a given pair of particles in the low-density limit only, where coalescence events involving more than two particles are negligible. Equation (9) shows that, in general, τ_B varies with time.

Now, at any given time, let τ' be the *shortest* collision time, i.e., the time at which the next binary collision will take place involving any pair among the $C_N^2 = \binom{N}{2}$ possible pairs of particles. Since the probability that any given particle will participate in that "next" collision is $p = (N-1)/\binom{N}{2} = 2/N$, the relation between τ_B and τ' is simply

$$\tau_B = \frac{N(t)}{2} \tau' \tag{10}$$

If multiple coalescence events have negligible weight, each collision will lower $N(t)$ by 1; hence

$$\langle m\rangle(t+\tau') = \frac{M_{\text{tot}}}{N(t)-1} = \frac{N(t)\langle m\rangle(t)}{N(t)-1} \tag{11}$$

Now, except at the very early stages of the irreversible evolution, $\tau' \ll t$, so that one may Taylor–expand the l.h.s. of Eq (11):

$$\langle m\rangle(t+\tau') \simeq \langle m\rangle(t) + \tau' \frac{d\langle m\rangle(t)}{dt} \simeq \langle m\rangle(t)\left[1+\frac{1}{N(t)}\right]$$

Hence

$$\frac{d\langle m\rangle(t)}{dt} = \frac{1}{\tau'}\frac{\langle m\rangle(t)}{N(t)} = \frac{\langle m\rangle(t)}{2\tau_{\text{B}}} \tag{12}$$

This result may be simply understood as follows: in a time interval τ_{B}, each cluster typically collides, leading to an increase of the average mass which is of the order of $\langle m\rangle(t)$ itself. The differential equation for $\langle m\rangle(t)$ cannot be solved unless the precise time dependence of τ_{B} is known. However, it is easily shown that a linear variation of τ_{B} is a necessary and sufficient condition for the existence of a scaling law (7a) of the mean mass. Indeed, if (7a) holds, then Eq. (12) implies

$$t^{\xi-1} \propto \frac{t^{\xi}}{\tau_{\text{B}}}$$

so that $\tau_{\text{B}} \propto t$. Conversely, if $\tau_{\text{B}} = At$, then, according to Eq. (12),

$$\frac{d\langle m\rangle(t)}{dt} = \frac{\langle m\rangle(t)}{2At}$$

which is easily solved to yield precisely (7a) with $\xi = 1/2A$.

3. MEAN-FIELD SCALING ANALYSIS

We now address the problem of estimating the scaling exponents ξ and δ. This will be achieved in the present section within the framework of a mean-field analysis physically equivalent to that of ref. 4. The key approximation which will be made throughout this analysis, either explicitly or implicitly, is to neglect any correlations between the initial momenta of particles which coalesce into a single sphere after a time t. This

assumption is likely to be wrong, since the momenta of the particles must satisfy certain constraints if they are to collide. Its degree of inadequacy may be expected to depend on dimensionality.

To estimate the kinetic energy exponent δ, consider an initial set of N spheres of mass m_0, r.m.s. speed v_0,and momenta $\{\mathbf{p}_i(0)\}(1 \leqslant i \leqslant N)$ which, at time t, merge into a single sphere of mass Nm_0, speed $v(t)$, and momentum $\mathbf{P}(t)$. According to momentum conservation (1c), the latter is given by

$$\mathbf{P}(t) = \sum_{i=1}^{N} \mathbf{p}_i(t) \tag{13}$$

Squaring Eq. (13) and taking a statistical average over all initial clusters of N particles that will merge into a single sphere of mass m at time t, one arrives at

$$\langle |\mathbf{P}(t)|^2 \rangle_m = \sum_{i=1}^{N} \langle |\mathbf{p}_i(0)|^2 \rangle_m + \sum_{i \neq j} \langle \mathbf{p}_i(0) \cdot \mathbf{p}_i(0) \rangle_m \tag{14}$$

Use of the mean-field assumption leads to

$$\langle |\mathbf{P}(t)|^2 \rangle_m \simeq \sum_{i=1}^{N} \langle |\mathbf{p}_i(0)|^2 \rangle_m = \frac{m}{m_0} \langle p_0^2 \rangle_m$$

or

$$\tfrac{1}{2} m \langle v^2 \rangle_m(t) \simeq \tfrac{1}{2} m_0 v_0^2 \tag{15}$$

Averaging next over all possible values of N (or equivalently m), one obtains

$$\tfrac{1}{2} \langle m v^2 \rangle(t) \simeq \tfrac{1}{2} m_0 v_0^2 \tag{16}$$

which simply expresses that the kinetic energy *per particle* (or aggregate) is conserved:

$$\langle \varepsilon \rangle(t) = \frac{K(t)}{N(t)} = \varepsilon_0 \tag{17}$$

Remembering the scaling relation (8b), this means that within the mean field approximation

$$\delta_{\mathrm{MF}} = \xi_{\mathrm{MF}} \tag{18}$$

The mean-field result (16), together with

$$\frac{\langle m \rangle(t)}{m_0} = \frac{n_0}{n(t)} \tag{19}$$

which follows directly from Eq. (5), show that the Boltzmann mean collision time (9) scales like

$$\tau_B \propto [\langle m \rangle(t)]^{\alpha} \tag{20}$$

where

$$\alpha = \tfrac{3}{2} - \nu(d-1) \tag{21}$$

Upon substitution of Eqs. (20) and (21) into Eq. (12), the differential equation may be easily solved; $\langle m \rangle(t)$ is found to increase according to the power law (7a), with the following mean-field estimate of exponent ξ:

$$\xi_{MF} = \frac{2}{3 - 2\nu(d-1)} \tag{22}$$

When $\nu = 1/d$, the result of Carnevale *et al.*,[4] $\xi_{MF} = 2d/(d+2)$, is recovered.

4. KINETIC THEORY AND HYPERSCALING RELATION

The exponent relation (18) and the value (22) for ξ rely on the mean-field assumptions. The latter seem to lead to correct results in 1D, where these predictions agree very well with computer simulation data.[4] In this section, we show that under much weaker assumptions, ξ and δ satisfy a hyperscaling relation which is more general than Eq. (18). Before presenting a more rigourous derivation of that relation, based on the exact kinetic equation governing the irreversible evolution of the distribution functions, a rough argument is given first, which rapidly leads to the correct results. The r.m.s. speed scales like

$$\langle v \rangle(t) \propto t^{\gamma} \tag{23}$$

where in view of the scaling relations (7a), (7b), the exponent gamma is easily seen to relate to δ as

$$\gamma = -\delta/2 \tag{24}$$

Substitution of (23), (7a), and (19) into expression (9) for the mean collision time shows that

$$\tau_B \propto t^{\xi - \gamma - \xi\nu(d-1)} \tag{25}$$

On the other hand, it was shown at the end of Section 2 that for a scaling law to exist for $\langle m \rangle$, τ_B must scale like t. It is immediately concluded that

$$\gamma + 1 = \xi[1 - (d-1)v] \tag{26}$$

A more satisfactory proof of this hyperscaling relation, which brings out its possible limitations, is based on the kinetic equation for the distribution function of masses and velocities. The mass m will be treated as a continuous variable rather than a discrete multiple of m_0, a reasonable assumption in the asymptotic regime when a broad distribution of masses has built up from a large number of coalescence events. Under these conditions, the one-particle distribution function for a spatially homogeneous system, $f^{(1)}(m, \mathbf{v}, t)$, is the probability density for finding particles with mass m and velocity $\mathbf{v}$ at time t. This function is related to higher order distribution functions by a BBGKY-like hierarchy.[10] If multiple coalescence events may be neglected, which is a valid assumption at sufficiently low densities, $f^{(1)}$ is exactly related to the two-particle distribution function:

$$f^{(2)}(m_1, \mathbf{v}_1, \mathbf{r}_1, m_2, \mathbf{v}_2, \mathbf{r}_2, t) = f^{(2)}(m_1, \mathbf{v}_1, m_2, \mathbf{v}_2, \mathbf{r}_2 - \mathbf{r}_1, t) \tag{27}$$

by the first equation of that hierarchy:

$$\begin{aligned} \frac{\partial f^{(1)}(m, \mathbf{v}, t)}{\partial t} = S_t(d) \int dm_1\, dm_2\, d\mathbf{v}_1\, d\mathbf{v}_2\, |\mathbf{v}_1 - \mathbf{v}_2| \left(\frac{\sigma_1 + \sigma_2}{2}\right)^{d-1} \\ \times \left\{ \delta(m - m_1 - m_2)\, \delta\left(\mathbf{v} - \frac{m_1 \mathbf{v}_1 + m_2 \mathbf{v}_2}{m}\right) \right. \\ \left. - \delta(m_1 - m)\, \delta(\mathbf{v}_1 - \mathbf{v}) - \delta(m_2 - m)\, \delta(\mathbf{v}_2 - \mathbf{v}) \right\} \\ \times f^{(2)}\left(m_1, \mathbf{v}_1, m_2, \mathbf{v}_2, \frac{\sigma_1 + \sigma_2}{2}, t\right) \end{aligned} \tag{28}$$

In Eq. (28), $S_t(d)$ is the total cross section of a particle of unit diameter ($S_t = 1,2$, and π in 1, 2, and 3 dimensions, respectively). The two-particle distribution function appearing in the collision integral of Eq. (28) is taken at contact, i.e., when the centers of the two colliding particles are at distances equal to the sum of their radii. In writing Eq. (28), it was assumed-for the sake of simplicity that the system is spatially homogeneous as expressed by Eq. (27). The kinetic equation (28) expresses the usual gain–loss balance; if coalescence events involving more than two particles became important, additional collision integrals involving higher order distribution functions $f^{(3)}, \ldots$ would be needed. Keeping in mind Eqs. (7a), (8a), and

(23), we make the following self-similarity assumptions regarding the time dependence of the one- and two-partiele distribution functions:

$$f^{(1)}(m, \mathbf{v}, t) = \frac{1}{t^{\alpha_1}} \tilde{f}^{(1)}\left(\frac{m}{t^{\xi}}, \frac{\mathbf{v}}{t^{\gamma}}\right) \tag{29a}$$

$$f^{(2)}(m_1, \mathbf{v}_1, \mathbf{r}_1, m_2, \mathbf{v}_2, \mathbf{r}_2, t) = \frac{1}{t^{\alpha_2}} \tilde{f}^{(2)}\left(\frac{m_1}{t^{\xi}}, \frac{\mathbf{v}_1}{t^{\gamma}}, \frac{m_2}{t^{\xi}}, \frac{\mathbf{v}_2}{t^{\gamma}}, \frac{|\mathbf{r}_1 - \mathbf{r}_2|}{t^{\xi/d}}\right) \tag{29b}$$

where $\tilde{f}^{(1)}$ and $\tilde{f}^{(2)}$ are scaling functions which do not explicitly depend on time. Conservation of the total mass implies

$$\int_0^{\infty} dm \int d\mathbf{v}\, m f^{(1)}(m, \mathbf{v}, t) = n_0 m_0 \tag{30}$$

Substitution of the self-similarity form (29a) into (30) immediately leads to the following value of the exponent α_1:

$$\alpha_1 = 2\xi + d\gamma \tag{31}$$

To determine α_2 it is sufficient to express that $f^{(2)}$ factorizes when the two particles are far apart, according to

$$f^{(2)}(m_1, \mathbf{v}_1, \mathbf{r}_1, m_2, \mathbf{v}_2, \mathbf{r}_2, t) \xrightarrow{|\mathbf{r}_1 - \mathbf{r}_2| \to \infty} f^{(1)}(m_1, \mathbf{v}_1, t) f^{(1)}(m_2, \mathbf{v}_2, t)$$

which can only be satisfied by the self-similar expressions (29a), (29b), provided that

$$\alpha_2 = 2\alpha_1 = 4\xi + 2d\gamma \tag{32}$$

If (29a) and (29b) are now substituted into the kinetic equation (28), the hyperscaling relation (26) follows. The mean-field values (22) and (18) of the exponents ξ and δ satisfy this relation identically.

5. UNIVERSAL DISTRIBUTION OF MASSES

The instantaneous mass distribution function $f(m, t)$ can be derived from the one-particle distribution function $f^{(1)}(m, \mathbf{v}, t)$ by integrating over velocities $\mathbf{v}$. Carrying out this integration on both sides of the hierarchy equation (28), one arrives at the following kinetic equation for $f(m, t)$:

$$\frac{\partial f(m, t)}{\partial t} = \int dm_1\, dm_2 \{\delta(m - m_1 - m_2) - \delta(m - m_1) - \delta(m - m_2)\} \times \nu_2(m_1, m_2, t) \tag{33}$$

where the collision frequency per unit volume $v_2(m_1, m_2, t)$ between particles of mass m_1 and m_2 is a functional of $f^{(2)}$; its explicit form immediately follows from inspection of the r.h.s. of Eq. (28), but will not be needed here.

Following Piasecki,[6] we close the kinetic equation by making the "weak" mean-field assumption:

$$v_2(m_1, m_2, t) = \frac{f(m_1, t)}{n(t)} \frac{f(m_2, t)}{n(t)} v(t) \tag{34}$$

where $v(t)$ denotes the total collision frequency per unit volume, while

$$n(t) = \int_0^\infty f(m, t)\, dm \tag{35}$$

is the instantaneous number density $N(t)/\Omega$. The factorization (34) does not preclude strong correlations between the velocities of particles about to collide.

The set of equations (33) and (34) gives rise to a closed nonlinear integrodifferential equation, since upon integration over m, Eq. (33) leads back to

$$\frac{dn(t)}{dt} = -v(t)$$

The problem may be solved by Laplace transformation, with the result[6]

$$f(m, t) = \frac{n(t)}{\langle m \rangle(t)} \exp\left(-\frac{m}{\langle m \rangle}\right) = \frac{n_0 m_0}{[\langle m \rangle(t)]^2} \exp\left(-\frac{m}{\langle m \rangle}\right) \tag{36}$$

which shows that the mass distribution function is a universal exponential function which scales with the instantaneous mean mass $\langle m \rangle(t)$; the form (36) is valid in the asymptotic regime $\langle m \rangle(t) \gg m_0$, irrespective of the initial distribution of masses. The result, initially derived by Piasecki[6] in 1D, is in fact valid for any dimension, provided multiple coalescence events may be neglected, and the weak mean-field assumption is valid.

6. SIMULATION OF THE TWO-DIMENSIONAL SYSTEMS

The predictions of mean-field theory have been tested for the one-dimensional system of coalescing point masses by extensive simulations reported in ref. 4, and excellent agreement was found, in particular as regards the values of the exponents ξ and $\delta(\xi = \delta = 2/3)$. However, the 1D case is somewhat peculiar, since the size of the particles is irrelevant, and

coalescence events are strictly binary. For that reason, we have carried out detailed simulations of ballistic coalescence of disks moving in a plane. Two values of ν were considered, namely $\nu = 1/2$ (corresponding to "collapsed" chains in the polymer language) and $\nu = 3/4$ (corresponding to "swollen" polymer chains). The former case is the object of the present section, while the latter will be discussed in the following section.

The code used in the simulations closely resembles the molecular dynamics (MD) algorithm for hard disks.[11] N_0 nonoverlapping disks of diameter σ_0 and mass m_0 are placed in a square cell of area $S = L^2$ and periodic boundary conditions are imposed. Each disk is assigned an initial velocity drawn from some given distribution function $\phi(\mathbf{v})$. The disks are left to move freely (ballistic motion) until they collide. The colliding particles merge (coalesce) into a single disk of mass and diameter given by Eqs. (1a) and (3) and with velocity and CM given by Eqs. (1b) and (1c). The algorithm checks for possible multiple coalescence events which occur whenever the disk resulting from the merging of the colliding particle pair overlaps any additional particle in the neighborhood. If so, these particles are absorbed in turn, under the same rules (1a)–(1c) and (3). An initial table of collision times for all pairs of particles is then updated, and free-flight motion resumes until the next collision occurs .

This dynamical evolution conserves the total momentum of the system. Moreover, for $\nu = 1/2$, the conservation of mass implies conservation of the packing fraction, i.e., of the fraction of the total area S covered by the nonoverlapping disks. Omitting the factor $\pi/4$, we have

$$n^*(t) = \frac{1}{S}\sum_{i=1}^{N(t)} \sigma_i^2 = \frac{1}{S}\sum_{i=1}^{N(t)} \frac{m_i}{m_0}\sigma_0^2 = \frac{1}{S}\frac{\sigma_0^2}{m_0} N_0 m_0 = n_0^* \tag{37}$$

It is important to realize that the mean free path of the particles increases with time. Indeed, exploiting Eq. (37), we obtain

$$l \propto \frac{1}{n(t)\langle\sigma\rangle(t)} \propto \frac{\langle\sigma\rangle(t)}{n_0^*} \propto [\langle m\rangle(t)]^{1/2} \propto t^{\xi/2} \tag{38}$$

The system's evolution, in the course of the simulations, was monitored until $l \simeq L$; any subsequent evolution would obviously be strongly affected by finite-size effects. The situation is reminiscent of critical fluctuations close to a second-order phase transition: standard simulation techniques are useless in the critical range, i.e, for temperatures sufficiently close to the critical temperature, such that the correlation length becomes comparable to the size of the simulation cell. The difficulty may be overcome by appealing to finite-size scaling techniques,[12] but the translation of these ideas to

the present irreversible situation is far from obvious. In practice, the simulations were interrupted when $l = L/5$.

Simulations were carried out for samples containing initially $5 \times 10^3 \leqslant N_0 \leqslant 2 \times 10^5$ particles and reduced densities in the range $10^{-3} \leqslant n_0^* \leqslant 0.8$. Initial velocities were usually sampled from a Maxwellian distribution $\phi(\mathbf{v})$ at a temperature T_0. In most runs, an initial square lattice configuration was first allowed to melt and equilibrate by letting the system evolve according to elastic collision dynamics; several independent runs were made for most initial state points in order to detect any sensitivity of the subsequent irreversible evolution on initial positions and velocities, but no significant differences were observed. The Boltzmann mean collision time of the initial monodisperse state

$$\tau_0 = (m_0 \sigma_0^2 / \pi k_B T_0)^{1/2} / 2 n_0^*$$

served as a natural time scale throughout. The characteristics and key results are summarized in Table I. In all cases which were investigated, log–log plots of $\langle m \rangle$ and K versus t/τ_0; clearly exhibited a scaling regime extending over typically two decades in time. Representative examples are shown in Fig. 1. The slopes of the log–log plots yield the exponents ξ and δ which are listed in Table I (in all the text, log means log base 10). In practice, δ turns out to be more accurately determined (with an estimated relative statistical error of less than 2%) than ξ. Table I also lists the "theoretical" values of ξ deduced from the hyperscaling relation (26), which reduces in the case under consideration ($d = 2$ and $\nu = 1/2$) to $\xi = 2 - \delta$.

Table I. Evolution of the MD Estimates of the Exponents ξ and δ with the Initial Reduced Density n^* [a]

n^*	N_0	δ	ξ	ξth	Multiple coalescence (%)
0.001	99856	1.12	0.8	0.88	0.029
0.01	99856	1.12	0.85	0.88	0.23
0.01	199809	1.12	0.86	0.88	0.22
0.01	399424	1.12	0.85	0.88	0.23
0.05	99856	1.10	0.90	0.90	1.23
0.3	99856	1.02	0.91	0.92	11
0.5	99856	1.03	0.95	0.97	26
0.8	99856	1.0	1.0	1.0	66

[a] ξth is evaluated from the hyperscaling relation (26) and the measured δ. The weight of multiple coalescence is also shown: the percentage is the ratio (number of particles disappearing in multiple coalescence events)/N_0. The data are for a size–mass exponent $\nu = 1/2$.

Inspection of the results in Table I calls for the following comments:

- As expected, multiple coalescence events, which are very rare at low densities, become more and more important as the density increases, and are predominant at the highest packing fraction investigated.
- The exponents ξ and δ differ significantly from their mean-field values $\xi_{MF}=\delta_{MF}=1$ [cf. Eqs. (22) and (18)]. In particular, $\delta>\xi$, so that the kinetic energy per particle decreases in time [cf. Eq. (8b)] rather than being constant, as implied by the mean-field argument of Section 3; this clearly illustrates the breakdown of the validity of the mean-field assumptions in dimension $d>1$.
- The exponents ξ and δ are "nonuniversal," i.e., their values depend on the reduced density n^*. This may not be surprising, in view of the growing importance of multiple coalescence events. The exponents are seen

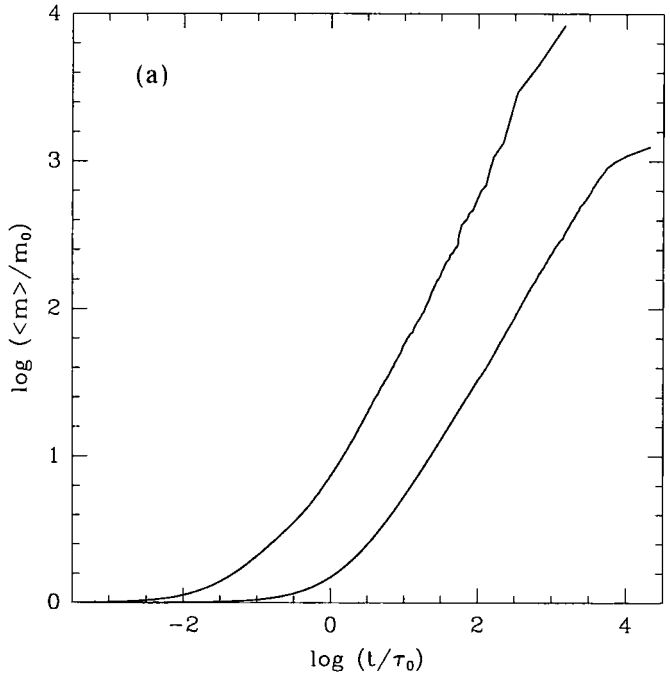

Fig. 1. (a) Plot of $\log(\langle m\rangle/m_0)$ vs. $\log(t/\tau_0)$ where τ_0 is the Boltzmann mean collision time at $t=0$ (which depends on n_0^*) and log means $\log_{10}$. Initial conditions: fluidlike configuration of $N_0 = 99856$ hard disks, with $n^*=10^{-2}$ and $n^*=0.8$ (upper curve). (b) Plot of $\log(K/K_0)$ vs. $\log(t/\tau_0)$. The dashed line represents the slope of $\log(K/K_0)$ vs. $\log(t/\tau_0)$ according to the mean-field result, with exponent δ_{MF}. Initial conditions: fluidlike configuration of $N_0=399424$ hard disks, with $n^*=10^{-2}$.

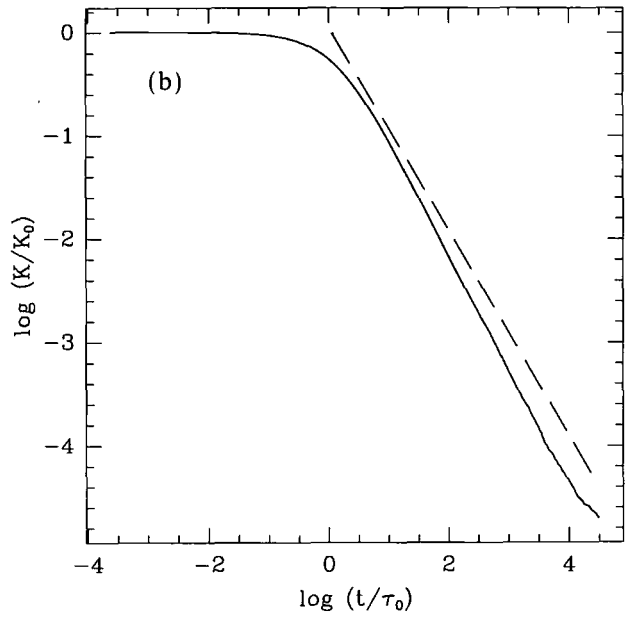

Fig. 1. (*Continued*)

to deviate most from their mean-field values at low densities, while they reduce to the mean-field values within statistical uncertainties at the highest density investigated. Multiple coalescence events thus appear to restore the validity of the assumption of lack of correlations between velocities of different disks about to merge into a single particle, and between velocities and masses. In the opposite low-density limit, it is tempting to conclude from our data that the exponents go over to universal limits ($\xi \simeq 0.88$; $\delta \simeq 1.12$) when multiple coalescence becomes statistically insignificant. It is difficult, however, to test this conjecture, since increasingly large system sizes would be needed in order to satisfy the constraint $l < L$ over a sufficiently long time interval required to probe the asymptotic scaling regime at very low densities.

• The hyperscaling relation $\xi = 2 - \delta$ is satisfied within statistical uncertainties at all densities. It is important to stress that the relation holds even outside the range of densities where the proof given in Section 4 is, strictly speaking, applicable.

As the irreversible evolution proceeds, the initially monodisperse system gradually evolves into a polydisperse system characterized by a

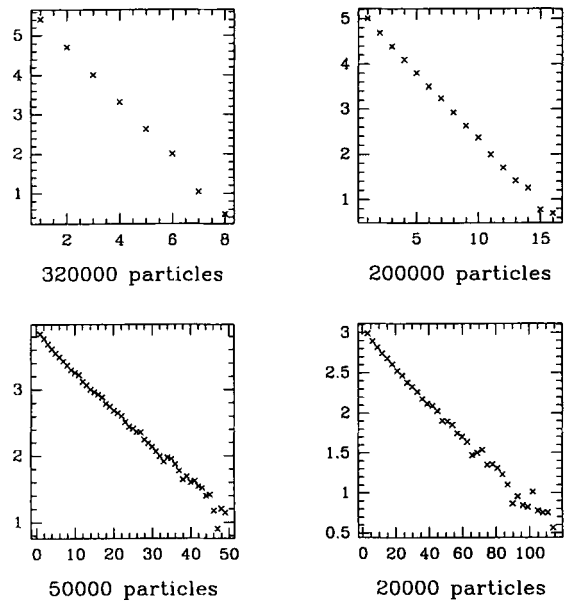

Fig. 2. Log of the mass distribution function versus m/m_0 at four successive times, when there are $N(t)$ particles left, as indicated ($N_0 = 399424$ and $n^* = 0.01$).

mass distribution $f(m, t)$, where m is an integer multiple of the initial mass m_0. In the continuum limit, it was shown in Section 5 that $f(m, t)$ is expected to be an exponential function of $m/\langle m\rangle(t)$, under rather weak assumptions. Typical histograms of the distribution of the integer values of m/m_0 are plotted in Fig. 2 at several stages of the irreversible evolution. At each stage, the logarithm of the distribution is well fitted to a straight line, so that one may express the distribution as

$$f(m, t) = \frac{1}{\beta(t)} \exp\left[-\frac{m}{M(t)} \right] \tag{39}$$

$M(t)$ and $\beta(t)$ differ from their values in the continuum limit by corrections due to discreteness; these corrections vanish in the asymptotic limit $M(t) \to \infty$, according to

$$\frac{\langle m\rangle}{M(t)} = 1 + \frac{m_0}{2M(t)} + o\left(\frac{m_0}{M(t)}\right) \tag{40a}$$

$$\frac{\beta(t) N_0}{M^2(t)} = 1 - \frac{m_0^2}{12M^2(t)} + o\left(\frac{m_0^2}{M^2}\right) \tag{40b}$$

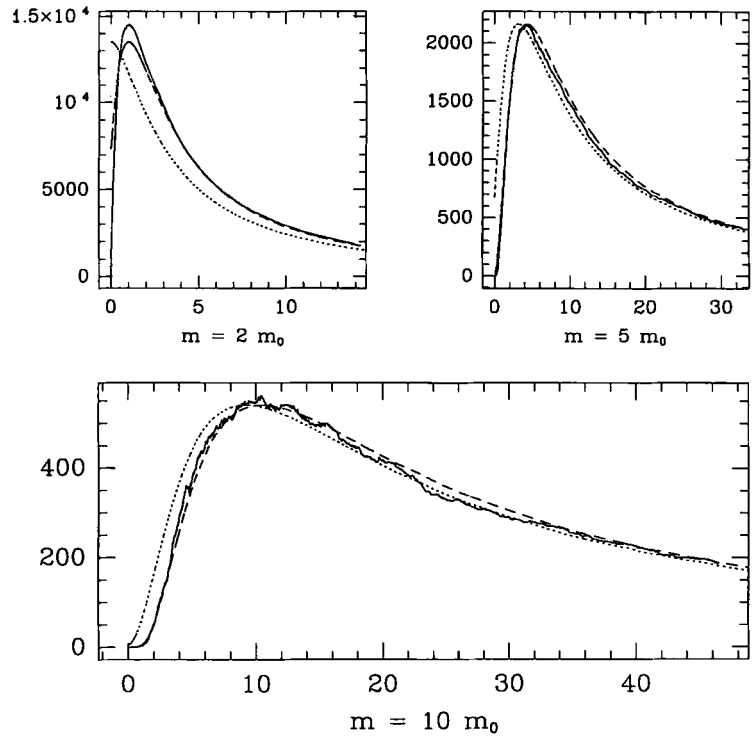

Fig. 3. $f(m, t)$ versus t/τ_0, for $m/m_0 = 2$, 5 and 10 ($n^* = 0.01$); simulation data are compared to the distribution function in the continuum limit (36) (dotted curve) and with the leading discreteness correction included [Eqs. (39), (40a), and (40b), dashed curve].

The influence of the discreteness of the mass spectrum is illustrated in Fig. 3, where the evolution of the populations of masses $m/m_0 = 2$, 5, and 10 is plotted versus time. As expected, corrections due to discreteness are significant only for the lowest mass.

Figure 4 shows the time evolution of the instantaneous mass structure factor:

$$S_{mm}(\mathbf{k}, t) = \frac{1}{N_0 m_0^2} |\rho_{\mathbf{k}m}(t)|^2 \tag{41}$$

where $\mathbf{k}$ is a wave vector compatible with the periodic boundary conditions, and $\rho_{\mathbf{k}m}(t)$ is the corresponding Fourier component of the instantaneous mass density:

$$\rho_{\mathbf{k}m}(t) = \sum_{i=1}^{N(t)} m_i e^{i\mathbf{k}\cdot\mathbf{r}_i(t)} \tag{42}$$

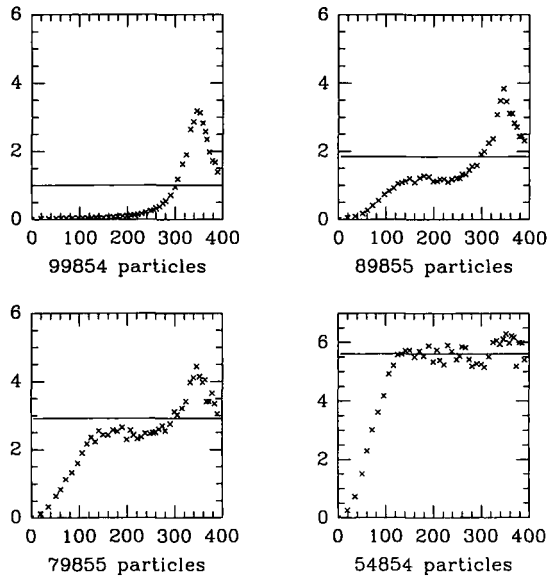

Fig. 4. $S_{mm}(\mathbf{k},t)$ versus k at four stages of the irreversible evolution. The straight line represents the aymptotic value ($k \to \infty$) of $S_{mm}(\mathbf{k}, t)$. k is given in units $2\pi/L$, where $2\pi/\sigma_0 = 353$. The initial configuration is a fluid of $N_0 = 99856$ hard disks with $n^* = 0.8$.

In order to achieve better statistics, the structure factor (41) was averaged for each value of $|\mathbf{k}|$ over five different vectors having the same modulus in the first Brillouin zone, and then coarsened over 50 different successive moduli. Initially, $S_{mm}(\mathbf{k},t)$ reduces to the equilibrium structure factor of a fluid of equal-size hard disks. As the system evolves, the increasing degree of polydispersity reflects itself in the appearance of a broad pre-peak, which grows at the expense of the initial main peak centered around $2\pi/\sigma_0$. At longer times, the structure is gradually washed out by polydispersity, except at the smallest wavenumbers k, where $S_{mm}(\mathbf{k}, t)$ drops to a rather small value related to the compressibility of the polydisperse fluid. The asymptotic ($k \to \infty$) value of $S_{mm}(\mathbf{k}, t)$ is equal to $N(t)\langle m^2\rangle(t)/m_0^2$, and hence increases like t^{ξ} in the scaling regime.

Another key quantity which was investigated in the simulations is the instantaneous distribution function of kinetic energies $f(\varepsilon, t)$, defined as

$$f(\varepsilon, t) = \frac{1}{n(t)} \iint \frac{1}{2} m v^2 f^{(1)}(m, \mathbf{v}, t)\, dm\, d\mathbf{v} \tag{43}$$

where $f^{(1)}$ is the one-particle distribution function introduced in Section 4.

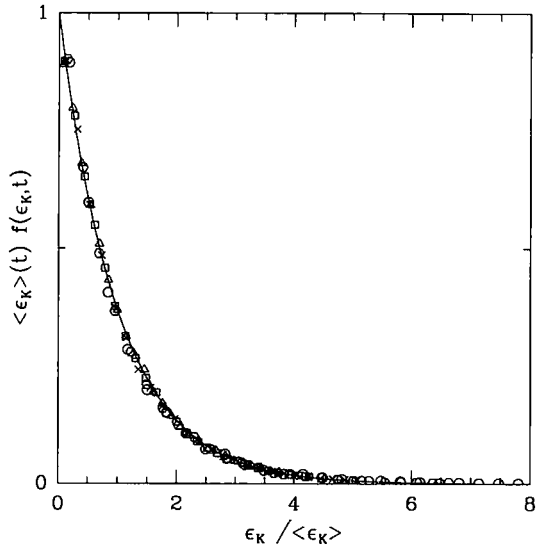

Fig. 5. Plots of $\langle\varepsilon\rangle f(\varepsilon, t)$ vs. $\varepsilon/\langle\varepsilon\rangle$ for $N_0 = 99856$ and $n^* = 10^{-3}$. The symbols correspond to $N(t) = 87000$ (triangles), 67000 (squares), 47000 (crosses), 27000 (hexagons), and 17000 (circles) particles left. The curve represents $\tilde{f}(x) = \exp(-x)$.

Starting from an initially well-equilibrated sample, characterized by a Maxwellian distribution at a temperature T_0, $f(\varepsilon, t)$ turns out to remain exponential to a high degree of accuracy at all times; the instantaneous temperature $T(t)$ derived from the slope of $\log f(\varepsilon, t)$ versus ε is found to agree perfectly with the kinetic temperature derived from the mean kinetic energy [cf. Eq (6)]. These findings are illustrated in Fig. 5 where the values of $\langle\varepsilon\rangle(t) f(\varepsilon, t)$, measured at five successive times, are plotted versus $\varepsilon/\langle\varepsilon\rangle(t)$. The data are seen to collapse on a single master curve $\tilde{f}(x)$ which is practically indistinguishable from an exponential, confirming that

$$f(\varepsilon, t) = \frac{1}{\langle\varepsilon\rangle(t)} \tilde{f}\left(\frac{\varepsilon}{\langle\varepsilon\rangle(t)}\right) \tag{44}$$

with $\tilde{f}(x) = \exp(-x)$. We conclude that at every stage of the evolution, the system is characterized by a Boltzmann distribution of energies, and hence appears to remain constantly in a state of local thermodynamic equilibrium. Even more remarkable is the observation that the energy distribution function evolves toward a Boltzmann distribution, when the initial distribution is highly non-Maxwellian. A typical example is shown in Fig. 6, where the initial distribution $f(\varepsilon, t = 0)$ has been chosen to increase linearly with ε up to ε_0. A tail at $\varepsilon > \varepsilon_0$ is seen to build up rapidly, while low-energy

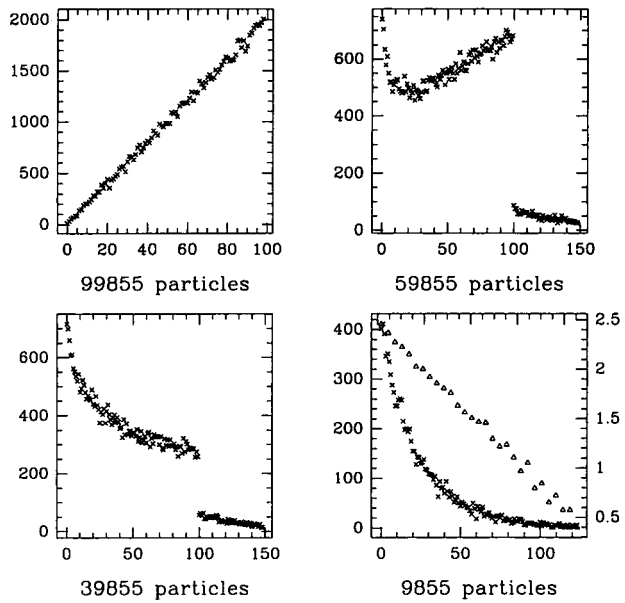

Fig. 6. $f(\varepsilon, t)$ versus ε at four different stages of the evolution in the case of an initial "sawtooth" distribution of energies ($N_0 = 99856$ with $n^* = 0.01$). In the last snapshot, a log-linear plot has been added to emphasize the Boltzmann nature of the energy distribution function [$\log f(\varepsilon, t)$ versus ε, triangles right-hand scale].

states are gradually populated. Before the end of the irreversible evolution, at a stage where about 10^4 particles are left, the distribution $f(\varepsilon, t=0)$ has returned to an exponential Maxwell–Boltzmann form. Such a behavior is the rule for a system relaxing toward a state of thermodynamic equilibrium, but is unexpected in a system far from equilibrium, which moreover does not conserve total energy. The "thermalization" shown in Fig. 6 was observed as well for other initial energy distributions differing from a Maxwell–Boltzmann distribution.

Finally, the mean square displacement of tagged particles was monitored to characterize the self-diffusion of particles gradually coalescing with others to form larger and larger particles. In the limit of elastic collisions (rather than inelastic coalescence) the mean square displacement would increase linearly according to Einstein's law:

$$\langle |\mathbf{r}(t) - \mathbf{r}(0)|^2 \rangle = 4Dt \tag{45}$$

discarding any logarithmic corrections expected in 2D systems, and associated with a slow t^{-1} decay of correlations (see, e.g., ref. 13).

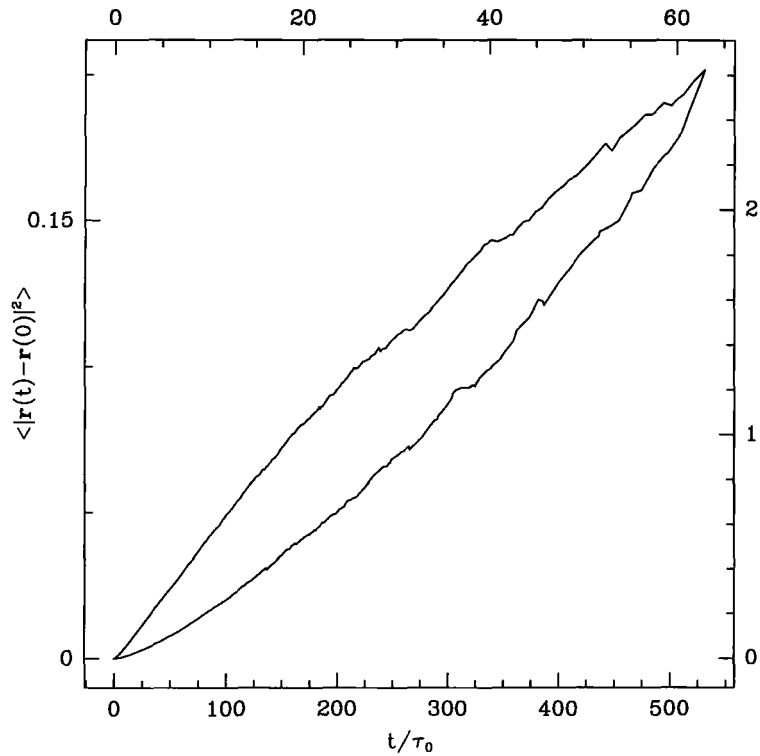

Fig. 7. $\langle|\mathbf{r}(t)-\mathbf{r}(0)|^2\rangle$ (averaged over all particles present at time t) vs. t/τ_0, for a low ($n^* = 10^{-2}$, upper curve, left-hand scale) and a high density ($n^* = 0.8$, lower curve, right-hand scale).

Plots of mean square displacements (averaged over all particles present at time t) versus time for the coalescence dynamics considered in the present work are shown in Fig. 7 for two densities. The mean square displacement appears to increase more slowly than linearly at the lower density (subdiffusive behavior), while, on the contrary, superdiffusive behavior seems to occur at the higher density. However, these observations should only be considered as indicative, since the results in Fig. 7 are based on a single irreversible history. Averaging over many initial conditions would require a much larger computational effort.

7. CATASTROPHIC GROWTH

We have also examined the case where the exponent ν in the size–mass relation takes on its Flory value $\nu = 3/(d+2)$, corresponding to "swollen"

chains in the polymer language. In that case, the mean-field estimate of the mean mass exponent ξ is, according to Eq. (22),

$$\xi_{MF}=\frac{2(d+2)}{3(4-d)} \tag{46}$$

This hints at the nonexistence of a scaling regime for dimensions $d \geqslant 4$. The instantaneous packing fraction $n^*(t)$, rather than being constant as in the case $\nu = 1/d$, is now expected to increase with time, according to

$$n^*(t)=\frac{1}{\Omega}\sum_{i=1}^{N(t)}\sigma_i^d \propto t^{2\xi(d-1)/(d+2)} \tag{47}$$

The increase in packing fraction means that multiple coalescence events become more and more probable as time evolves. Since the results of the previous section clearly suggest that the exact scaling law exponents ξ and δ change with packing fraction, it is not clear whether a clear-cut scaling regime exists for the "swollen chain" case. Also, since $n^*(t)$ cannot increase beyond close packing, one expects that the irreversible coalescence of particles terminates in a final "catastrophic" event involving all remaining

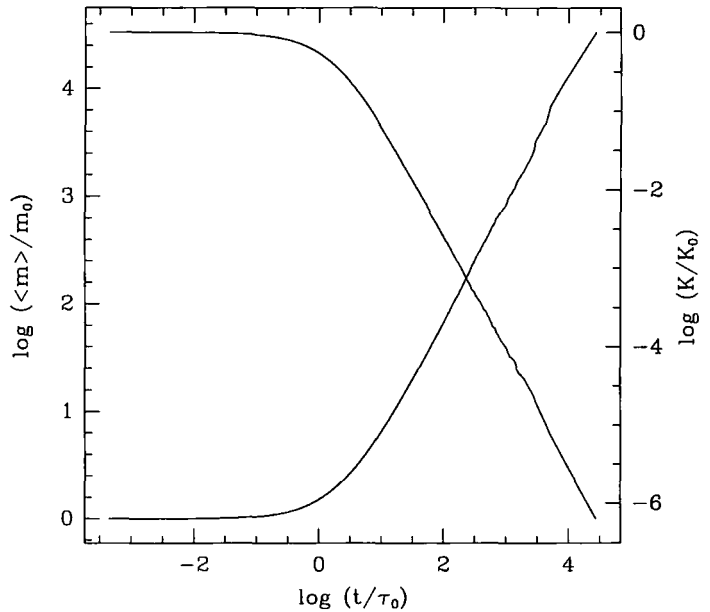

Fig. 8. Plots of $\log(\langle m\rangle/m_0)$ (left-hand scale) and $\log(K/K_0)$ (right-hand scale) vs. $\log(t/\tau_0)$ for the Flory case ($d=2$, $\nu=3/4$); $n_0^*=10^{-3}$.

particles. The occurrence of such a "catastrophe" may be avoided for any given initial number of particles N_0 provided the initial reduced density $n_0^* = N_0 \sigma_0^d / \Omega$ is less than a critical value n_{0c}^*. The latter may be roughly estimated by expressing that in the final state of the irreversible evolution, all initial particles have merged into a single sphere of mass $N_0 m_0$ and diameter $\Sigma = N_0^{\nu} \sigma_0$, which can at most be equal to the edge $L = \Omega^{1/d}$ of the system volume. This leads immediately to the estimate

$$n_{0c}^* = N_0^{1-\nu d} \tag{48}$$

In order to explore the possible scenarios, we have carried out MD simulations on 2D samples of $N_0 = 2 \times 10^5$ initial particles. With $\nu = 3/4$, Eq. (48) then leads to the estimate $n_{0c}^* = N_0^{-1/2} \simeq 0.0022$. We have accordingly studied the cases with initial reduced density $n_0^* = 0.001$, $n_0^* = 0.003$, and $n_0^* = 0.01$. Log–log plots of mean mass and of the total energy versus time are shown in Fig. 8 for $n_0^* = 10^{-3}$. A clear-cut scaling regime is observed over more than two decades, and the resulting exponents have the values $\xi = 1.10$ and $\delta = 1.44$, which differ considerably from the mean-field values $\xi_{MF} = \delta_{MF} = 4/3$. The scaling relation (26), which reads $\xi = 4 - 2\delta$ in the present case, is very well obeyed.

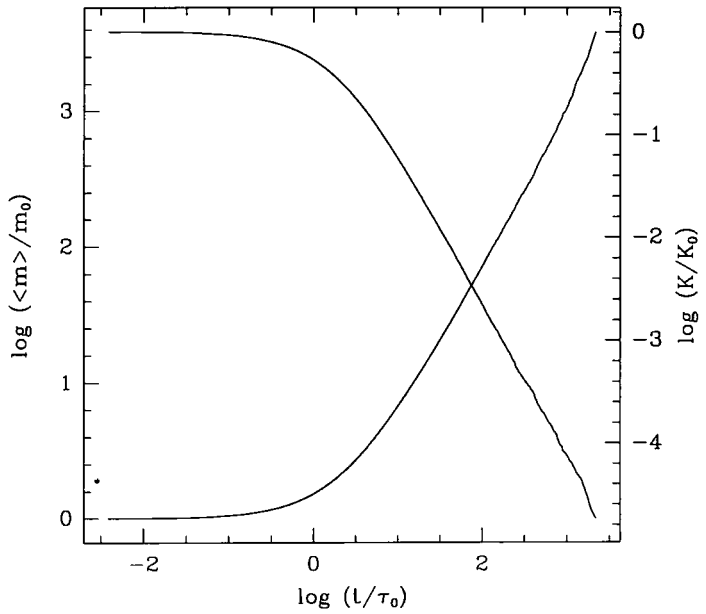

Fig. 9. Same as Fig. 8, for $n_0^* = 3 \times 10^{-3}$.

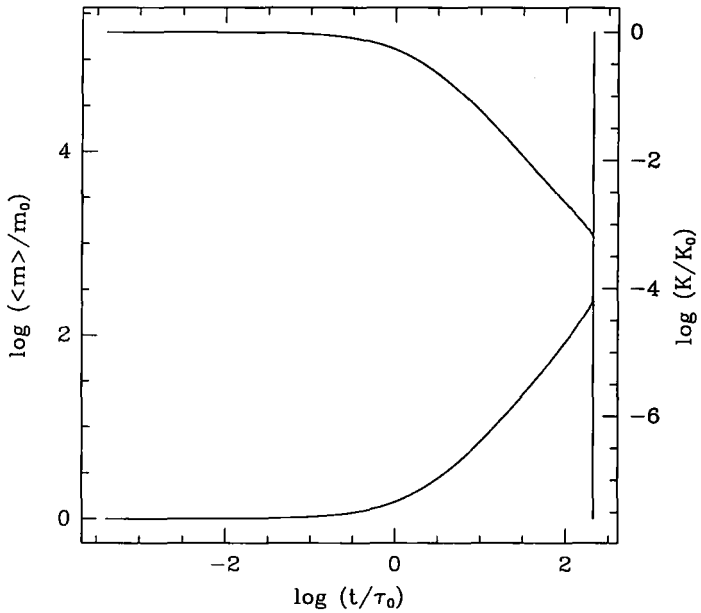

Fig. 10. Same as Fig. 8, for $n_0^* = 3 \times 10^{-2}$. The evolution terminates in a final coalescence event involving all $N(t) = 830$ particles.

The corresponding results for $n_0^* = 0.003$ are shown in Fig. 9. In this case, no genuine scaling regime is observed; the exponents δ and ξ appear to change gradually as the packing fraction increases, as suggested above. A similar remark holds for $n_0^* = 0.01$ (cf. Fig. 10), but in this case, the evolution terminates in a "catastrophic" multiple coalescence event, at a stage where 800 particles are left and the reduced density has reached the value $n^* \simeq 0.25$. This brutal transition is vaguely reminiscent of a sol–gel transition in polymer solutions. The transition is reproducible, in the sense that it is observed to occur at the same stage of the evolution for different initial conditions.

8. CONCLUSION

The dynamic scaling behavior of ballistic coalescence is richer and more complex than surmised from mean-field arguments and the results of simulations of 1D systems. Considering first the coalescence into compact ("collapsed") particles, the most important conclusion of the present work on 2D systems is the confirmation of the existence of a well-defined scaling regime, but with mass and energy exponents which are nonuniversal, since

they turn out to depend on packing fraction. This may be traced back to the increasing weight of multiple coalescence events, which are absent in 1D. As the density is lowered, these events become rarer, and the exponents ξ and δ converge toward limiting values which differ significantly from the prediction on mean-field theory (this seems to be at variance with the conjecture put forward by ref. 5). These limiting values satisfy a hyperscaling relation which follows from the exact kinetic equation for the distribution function, and a self-similarity assumption. The hyperscaling relation, which, strictly speaking, is justified in the low-density (binary coalescence) limit only, continues to be satisfied by the measured exponents up to high densities, where these exponents appear to return to their mean-field values.

The mass distribution is found to be exponential and universal to a high degree of accuracy, in agreement with a prediction derived from a "weak" mean-field assumption. The energies are also distributed according to a Boltzmann distribution at all times, and, more surprisingly, the nonequilibrium system is found to thermalize (with a time-dependent temperature) even when the initial distribution of velocities is highly non-Maxwellian.

In the other case investigated here, when the size–mass relation corresponds to "swollen" objects, a scaling regime is observed only when the initial packing fraction is sufficiently low. At higher values of n_0^*, the irreversible evolution terminates in a final "catastrophic" multiple coalescence event.

The present model may be regarded as providing a highly schematic description of polymerization or colloid growth. However, the assumption of ballistic motion between coalescence events is not suitable for phenomena which are essentially diffusion controlled. For that reason we are presently considering a variant of the model where the particles are undergoing Brownian (rather than free) motion between collisions. The simulation work will also be extended to 3D, where deviations from mean-field behavior may be even more pronounced.

ACKNOWLEDGMENTS

The authors acknowledge helpful discussion with L. Bocquet, J. Piasecki, and W. Young, and are grateful to a referee for attracting their attention to ref. 5. The simulations were carried out under the auspices of the Pôle Scientifique de Modélisation Numérique at École Normale Supérieure de Lyon. J.P.H. acknowledges the hospitality of the Physical and Theoretical Chemistry Laboratory, and Balliol College, Oxford.

REFERENCES

1. T. A. Witten and L. M. Sanders, *Phys. Rev. Lett.* **47**:1400 (1981).
2. P. Meakin, In *Phase Transitions and Critical Phenomena*, Vol. 12, C. Domb and J. L. Lebowitz, eds. (Academic Press, London, 1988).
3. P. Meakin, *Rep. Prog. Phys.* **55**:157 (1992).
4. G. F Carnevale, Y. Pomeau, and W. R. Young, *Phys. Rev. Lett.* **64**:2913 (1990).
5. Y. Jiang and F. Leyvraz, *J. Phys. A* **26**:L179 (1993).
6. J. Piasecki, *Physica A* **190**:95 (1992).
7. Ph. A. Martin and J. Piasecki, *J. Stat. Phys.* **76**:447 (1994).
8. E. Trizac and J. P. Hansen, *Phys. Rev. Lett.* **74**:4114 (1995).
9. P. J. Flory, *Principles of Polymer Chemistry* (Cornell University Press, Ithaca, New York, 1953).
10. S. Chapman and T. J. Cowling, *The Mathematical Theory of Non-Uniform Gases*, 3rd ed. (Cambridge University Press, Cambridge, 1970); P. Résibois and M. De Leener, *Classical Kinetic Theory of Fluids* (Wiley, New York, 1977).
11. B. J. Alder and T. E. Wainwright, *J. Chem. Phys.* **31**:459 (1959).
12. N. M. Barber, In *Phase Transitions and Critical Phenomena* Vol. 8, C. Domb and J. L. Lebowitz, eds. (Academic Press, London, 1983).
13. Y. Pomeau and P. Résibois, *Phys. Rep.* **19**:63 (1975).